https://doi.org/10.5194/egusphere-2024-1652
Preprint. Discussion started: 5 June 2024

Tropospheric Links to Uncertainty in Stratospheric Subseasonal Predictions

Rachel W.-Y. Wu[1], Gabriel Chiodo[1], Inna Polichtchouk[2], and Daniela I.V. Domeisen[3,1]

[1]Institute for Atmospheric and Climate Science, ETH Zurich, Zurich, Switzerland
[2]European Centre for Medium-Range Weather Forecasts, Reading, UK
[3]Faculty of Geosciences and Environment, University of Lausanne, Lausanne, Switzerland

Correspondence: Rachel W.-Y. Wu (rachel.wu@env.ethz.ch)

Abstract. Variability in the stratosphere, especially extreme events such as Sudden Stratospheric Warmings (SSWs), can impact surface weather. Understanding stratospheric prediction uncertainty is therefore crucial for skillful surface weather forecasts on weekly to monthly timescales. Using ECMWF subseasonal hindcasts, this study finds that stratospheric uncertainty is most strongly linked to tropospheric uncertainty over the North Pacific and Northern Europe, regions that can modulate but also respond to stratospheric variability, suggesting a two-way propagation of uncertainty. A case study of the 2018 SSW event shows an initial poleward and upward propagation of uncertainty from tropical convection, followed by a downward propagation where ensemble members that accurately predict the SSW also better at predicting its downward impacts. These findings highlight the locations in the troposphere that are linked to stratospheric uncertainty and suggest that improved model representation of tropospheric mechanisms linked to polar vortex variability could enhance both stratospheric and extratropical surface prediction.

1 Introduction

Anomalous variability in the stratosphere is an important precursor for surface weather anomalies (Baldwin and Dunkerton, 2001) and extremes (Domeisen and Butler, 2020) on weekly to monthly timescales in winter and spring. In particular, sudden stratospheric warming (SSW) (Baldwin et al., 2021) and strong vortex events are windows of opportunity for extended-range weather prediction (e.g. Domeisen et al., 2020b; Butler et al., 2018; Scaife et al., 2016). Indeed, the stratosphere has an extended predictability limit with respect to the troposphere (Domeisen et al., 2020a; Son et al., 2020). These longer characteristic timescales in the stratosphere suggest a potential for increased predictability of surface weather arising from stratospheric forcing, particularly on subseasonal-to-seasonal (S2S) timescales, ranging from weeks to months. However, when it comes to predicting the variability in the stratosphere in the first place, extreme stratospheric events, especially SSW events, have a more limited predictability as compared to more neutral states of the vortex, meaning that the average predictability of an SSW is around 5-10 days in dynamical models (Domeisen et al., 2020a; Taguchi, 2018; Chwat et al., 2022), indicating a higher uncertainty ahead of such events.

Uncertainty in the prediction of stratospheric variability can be contributed by model uncertainty in both the stratospheric mean state and in upward wave propagation (Tripathi et al., 2015a), as the strength of the stratospheric polar vortex is modulated

https://doi.org/10.5194/egusphere-2024-1652
Preprint. Discussion started: 5 June 2024

by the interaction of planetary waves with the stratospheric mean flow. The planetary waves entering the stratosphere can break, depositing wave momentum and thereby forcing a weakening of the westerly vortex winds. The breaking of planetary waves can also precondition the vortex into a state that is more favourable for wave propagation (Limpasuvan et al., 2004; Albers and Birner, 2014), which acts to guide waves towards the vortex (Matsuno, 1970), thus making the deposition of wave momentum more focused in the vortex area. Hence, the strength and geometry of vortex winds and upward wave propagation can strongly influence the subsequent evolution of the polar vortex. Model biases with respect to these details of the three-dimensional structure of the stratosphere - troposphere system can therefore strongly impact the uncertainty in the prediction of the stratosphere.

Subseasonal-to-seasonal forecast systems are subject to model biases in both polar vortex strength (Lawrence et al., 2022) and in tropospheric stationary waves (Schwartz et al., 2022), which interact with wave anomalies to determine the upward wave flux (Smith and Kushner, 2012). It has been suggested that the dominant factor in limiting the prediction of SSWs is the prediction of planetary wave activity rather than the mean state (Stan and Straus, 2009; Wu et al., 2022; Portal et al., 2022). The major sources of uncertainty in predicting the wave activity driving SSWs are suggested to be associated with the model representation of tropospheric stationary wave ridges in western North America and the North Atlantic region (Schwartz et al., 2022), and for individual SSW events, in the representation of extratropical blocking, as found for the 2018 SSW event (Karpechko et al., 2018; Lee et al., 2019; Statnaia et al., 2020), and localized synoptic-scale tropospheric perturbations, as shown by Kent et al. (2023) for the 2013 SSW event.

Through teleconnection pathways, variability in the tropics can contribute to uncertainty in the extratropics, which can further propagate into the stratosphere (Straus et al., 2023; Roberts et al., 2023). The Madden-Julian Oscillation (MJO), the dominant mode of intraseasonal variability in the tropics, influences the extratropics by modulating extratropical tropospheric stationary waves, over the North Pacific in particular, and can further impact the stratospheric polar vortex by exciting poleward and vertical wave propagation (Garfinkel et al., 2012, 2014). Model initializations that better capture the MJO show better prediction skill over the North Pacific and Euro-Atlantic region (e.g. Ferranti et al., 2018; Kim et al., 2023) and better upward coupling of the troposphere into the stratosphere (Stan et al., 2022), resulting in better simulation of SSWs (Schwartz and Garfinkel, 2020; Kang and Tziperman, 2018).

Uncertainty in the troposphere can also be a response to the extreme states of the polar vortex itself (e.g. Charlton et al., 2004; Sigmond et al., 2013; Tripathi et al., 2015b; Domeisen et al., 2020b). Forecast skill can be enhanced after stratospheric extreme events (Sigmond et al., 2013; Tripathi et al., 2015b), but can also be reduced since the forecasts can be overconfident (Büeler et al., 2020), in particular over Europe (Domeisen et al., 2020b). In particular, tropospheric internal variability can limit the coupling of stratospheric predictability to the troposphere. For instance, following the 2018 SSW event, the uncertainty in the development of synoptic activity after the SSW onset impacted the predictability of surface anomalies (González-Alemán et al., 2022).

Given that the uncertainty in the stratosphere is coupled to uncertainty in the troposphere, this study aims to systematically investigate the link between stratospheric and tropospheric uncertainty in the ECMWF subseasonal-to-seasonal (S2S) hindcasts and to identify regions and pathways for which better model representation might enhance the skill of stratospheric prediction.

https://doi.org/10.5194/egusphere-2024-1652
Preprint. Discussion started: 5 June 2024

2 Data and Methods

The Northern Hemispheric (NH) winter (November to February) subseasonal-to-seasonal (S2S) hindcasts (Vitart et al., 2017) of ECMWF model versions CY43R3 and CY45R1 are analyzed for the period 1998/99 to 2017/18. The hindcasts consist of 11 ensemble members, are integrated for 46 days and initialised twice a week. Both versions share similar configurations and are initialized with the ECMWF ERA-I reanalysis (Dee et al., 2011).

In addition, a hindcast for a case study initialized on 2018-01-27, 16 days before the onset of the 2018 SSW event, is chosen for a re-run to investigate the development of the large ensemble spread associated with this particular hindcast. The hindcast is computed for an increased ensemble size (51 members compared to 11 in the original hindcast) and for more pressure output levels to enable a more robust investigation of the spread. The hindcast is re-run using model version CY47R3, computed on 2022-01-27, and is initialized with ERA5 reanalysis (Hersbach et al., 2020). The daily means of the 20-year hindcasts of this model version, computed on the same calendar date on 2022-01-27, are chosen as the climatology to compute anomalies for the indcasts.

The zonal mean zonal wind at 60°N and 10 hPa (u1060) is used as a measure of the strength of the stratospheric polar vortex. As a measure of upward wave activity in the lower stratosphere, we use the zonal average of meridional eddy heat fluxes ($\overline{v'T'}$) averaged over 40-80° N at 100 hPa and weighted by the cosine of latitude, where v is the meridional wind, T is the temperature, and prime ($'$) denotes the departure from the zonal mean.

Hindcasts are categorized based on their ensemble spread in u1060. The uncertainty is estimated by first calculating the daily standard deviation of u1060 across the ensemble members of each hindcast. These daily standard deviations are then averaged over the 46-day integration period of the hindcast to obtain an estimate of the overall uncertainty present in the hindcast. Based on this 46-day average uncertainty, the hindcasts are separated into composites of large and small uncertainty, each consisting of 328 hindcasts. Specifically, the large uncertainty composite (large u1060 spread) is composed of hindcasts with an ensemble spread above the 75th percentile of all hindcasts (9.16 ms^{-1}), and the small uncertainty composite (small u1060 spread) is composed of hindcasts with an ensemble spread below the 25th percentile (5.86 ms^{-1}).

3 Uncertainty in the Ensemble Prediction of the Stratosphere

We start by comparing and characterizing the features of high and low uncertainty hindcasts in the ECMWF subseasonal-to-seasonal (S2S) model. Hindcasts that exhibit large uncertainty in the prediction of the strength of the stratospheric polar vortex (u1060) are associated with strong growth in the spread at around 5-25 days after initialization (Figure 1a). For hindcasts that exhibit small uncertainty, the spread in u1060 grows as lead time increases, but the rate of increase is much smaller than for the large uncertainty composite. Hereafter, the large uncertainty and small uncertainty composites are referred to as large u1060 spread and small u1060 spread composite, respectively.

The ensemble mean evolution in u1060 of the identified composites (Figure 1b) shows that on the day of initialization (day 0), the large u1060 spread hindcasts are more generally associated with a strong vortex and the small u1060 spread hindcasts are associated with a weak vortex, with the medians of the composites being 36.28 ms^{-1} and 13.25 ms^{-1} on day 0, respectively.

https://doi.org/10.5194/egusphere-2024-1652
Preprint. Discussion started: 5 June 2024

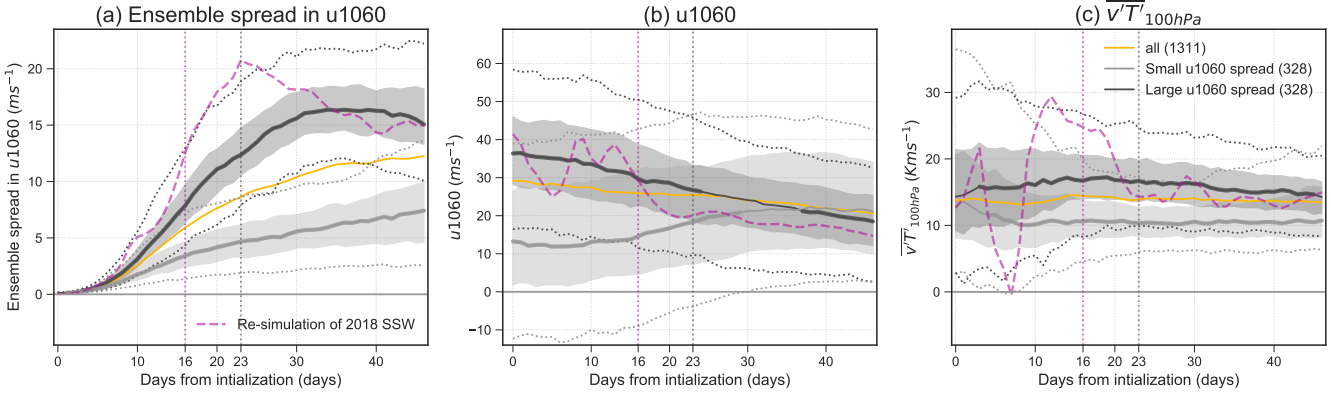

Figure 1. Evolution of (a) ensemble spread in u1060 and (b) ensemble mean of u1060 and (c) ensemble mean of $\overline{v'T'}$ at 100hPa in composites of hindcasts classified as having large uncertainty (large u1060 spread, black) and small uncertainty (small u1060 spread, grey), respectively, for the prediction of the stratospheric polar vortex. The solid line denotes the median, the shaded region denotes the 25th to 75th percentiles, and dotted lines denote the 5th and 95th percentiles, for the large and small spread composites. The median of all hindcasts is shown in yellow. Solid lines are printed in bold when the composites are significantly different from all hindcasts at the 95% confidence interval using a t-test. The ensemble spread and ensemble mean corresponding to the hindcast of the 2018 SSW event are plotted as purple dashed lines. Dotted vertical purple and grey lines indicate the onset and the peak of the uncertainty in $u1060$ for the 2018 SSW event, respectively. The number of hindcasts in each composite is given in brackets in the legend.

After day 0, the large u1060 spread composite shows an overall weakening of the vortex and the small u1060 spread composite shows an overall strengthening of the vortex. The u1060 evolution of the composites is likely related to the fact that SSWs or vortex weakenings in the large u1060 spread composite occur predominantly at relatively long lead times (from 10 days after initialization), while the SSWs or vortex weakenings in the small spread composite occur mostly at early lead times (within the first 10 days after initialization) (not shown). The difference in vortex strength between the composites reduces with lead time but remains significantly different from that of all hindcasts until 24 and 29 days after initialization, for the large and small u1060 spread composites, respectively. Towards longer lead times, from around 35 days after initialization, the composites display a vortex strength similar to all hindcasts, likely linked to the model's drift towards climatology at long lead times. After that, the small u1060 spread composite stagnates at a vortex strength similar to all hindcasts, while the large u1060 spread composite weakens further and show significantly weaker vortex strength than all hindcasts starting on day 37.

The respective behavior of the composites is consistent with our understanding that when the stratospheric mean flow is westerly, vertical wave propagation in the NH is possible for small wavenumbers (Charney and Drazin, 1961), while the exact propagation properties of the waves are modulated by the three-dimensional structure of the stratospheric flow. A strong vortex can further act as a waveguide, guiding waves from the troposphere towards the polar stratosphere (Matsuno, 1970; Simpson et al., 2009; Albers and Birner, 2014). On the other hand, when the vortex in the lower stratosphere is very weak, such as after an SSW event, waves can be inhibited from propagating upwards, and the vortex can strengthen radiatively (Limpasuvan et al.,

https://doi.org/10.5194/egusphere-2024-1652
Preprint. Discussion started: 5 June 2024

2005; Hitchcock and Shepherd, 2013). Indeed, as expected, the large u1060 spread composite that is associated with a stronger vortex is associated with stronger eddy heat flux in the lower stratosphere, as compared to the small u1060 spread composite, which is associated with a weaker vortex and weaker eddy heat flux (Figure 1b and c).

To better understand the regional contributions to the spread in u1060, we now investigate the longitudinal structure of the lower stratospheric heat flux (Figure 2). The large u1060 spread composite shows anomalously positive eddy heat flux over the North Pacific (NP), Northern Europe (NE), Siberia (Sib) and anomalously negative heat flux over North America (NA) (Figure 2a). The heat flux associated with NP peaks in the first few days after initialization, while that in the NA peaks after 10 days and in the NE after 15 days. For the small u1060 spread composite, the heat flux is weaker than for the large u1060 spread composite (Figure 2b) and comparable to the average of all hindcasts (yellow contours in Figure 2b). The heat flux of the small u1060 spread composite is strongest at initialization and gradually decreases within the first 10 days for all longitudes. Interestingly, the heat flux over the North Pacific of the small u1060 spread composite increases again around 25 days after initialization, which might explain the stagnation of the increase in $u1060$ for the small spread composite in Figure 1b. The largest difference in the ensemble mean heat flux between the composites is found over the North Pacific owing to the very strong positive heat flux over the North Pacific associated with the large u1060 spread composite (Figure 2c).

In terms of ensemble spread, the large u1060 spread composite shows large uncertainty in the heat flux in all regions that also exhibit a large ensemble mean heat flux (Figure 2d). For the small u1060 composite, uncertainty is found in the same regions as for the large u1060 composite, but the ensemble spread is much weaker (Figure 2e). The largest difference between the high and low spread composites in descending order is over Northern Europe, followed by North America, the North Pacific, and Siberia (Figure 2f).

4 Tropospheric Links to Stratospheric Uncertainty

As a next step, we investigate whether the uncertainty in the stratosphere is related to uncertainty in the troposphere by comparing the temporal and spatial evolution of the uncertainty of the large and small u1060 composites in mean sea level pressure (MSLP) anomalies (Figure 3). In the first 5 days after initialization, only small significant patches of larger uncertainty are found in the large u1060 spread composite compared to the small spread composite (Figure 3a). At days 5 - 10, a significant difference between the large and small u1060 spread composite is found over the North Pacific, the polar regions, Northern Europe and the Ural region. The difference in uncertainty between the composites at these regions persists and amplifies as lead time increases (Figure 3b - f), especially over the North Pacific and Scandinavia.

Other regions with significant differences between the large and small spread composites include the Azores High and the tropics during days 10 - 30 (Figure 3c - f). Smaller uncertainty is found in the large u1060 spread composite than the small u1060 spread composite over the Azores High during days 10 - 25 (Figure 3c - e). In the tropics, a small but significant difference is found from days 10 - 15 over the Maritime Continent and the tropical Pacific Ocean where the large u1060 spread composite shows larger uncertainty than the small u1060 composite (Figure 3c). The difference in uncertainty between the

https://doi.org/10.5194/egusphere-2024-1652
Preprint. Discussion started: 5 June 2024

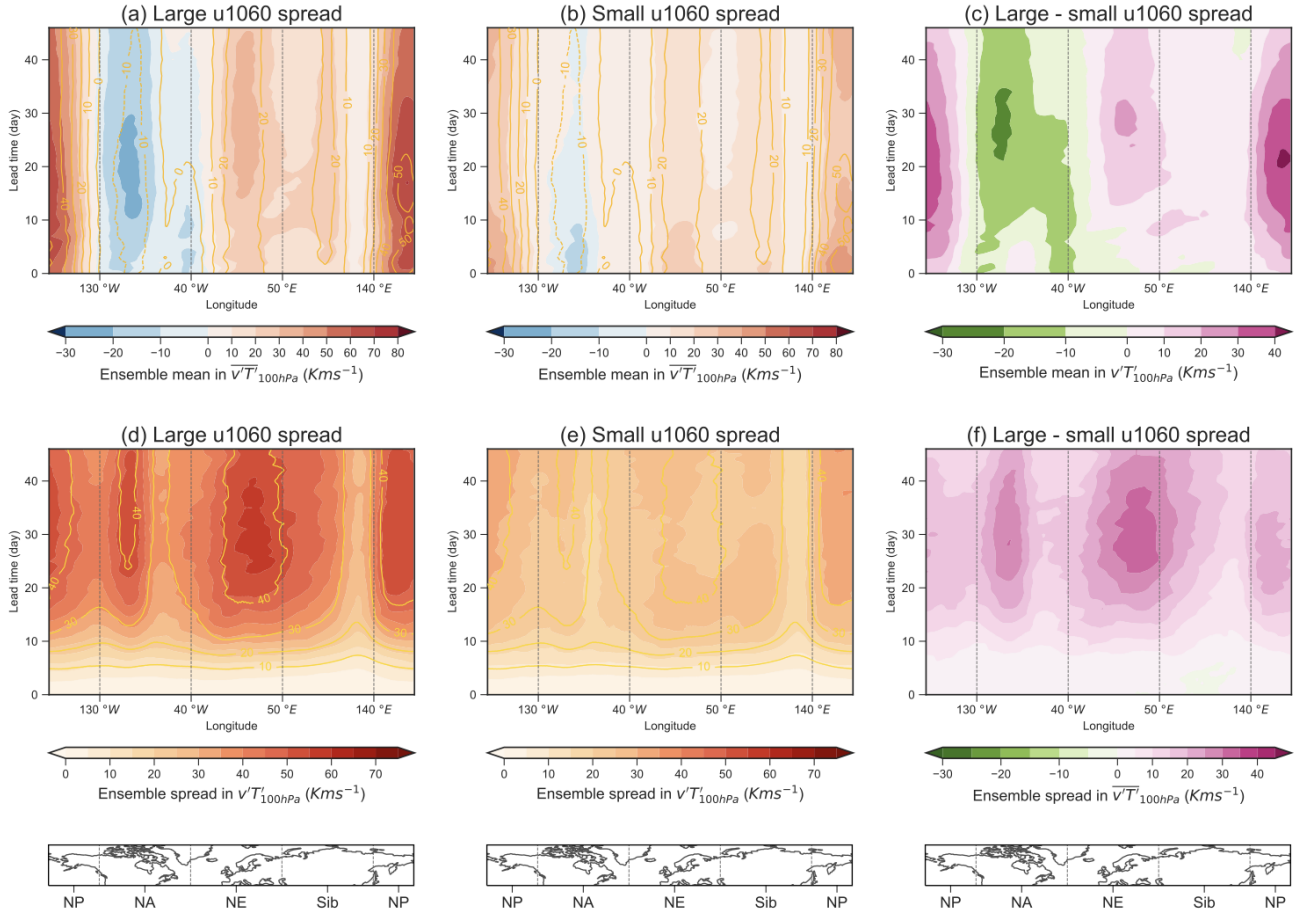

Figure 2. Hovmöller diagrams of composite ensemble mean and ensemble spread of $v'T'$ at 100hPa for (a,d) hindcasts with large spread in u1060 and (b,e) hindcasts with small spread in u1060. The difference between the composites, given as large minus small spread composite, in the ensemble mean and ensemble spread is displayed in (c) and (f), respectively. The averages over all hindcasts are plotted in yellow contours. The grey vertical lines separate the regions of investigation, from left to right: North Pacific (NP, 140°E - 130°W), North America (NA, 130°W - 40°W), Northern Europe (NE, 40°W - 50°E) and Siberia (Sib, 50°E - 140°E). Note that the negative range of the colorbars is smaller than the positive range for visualisation purposes, but the contour levels are kept constant.

https://doi.org/10.5194/egusphere-2024-1652
Preprint. Discussion started: 5 June 2024

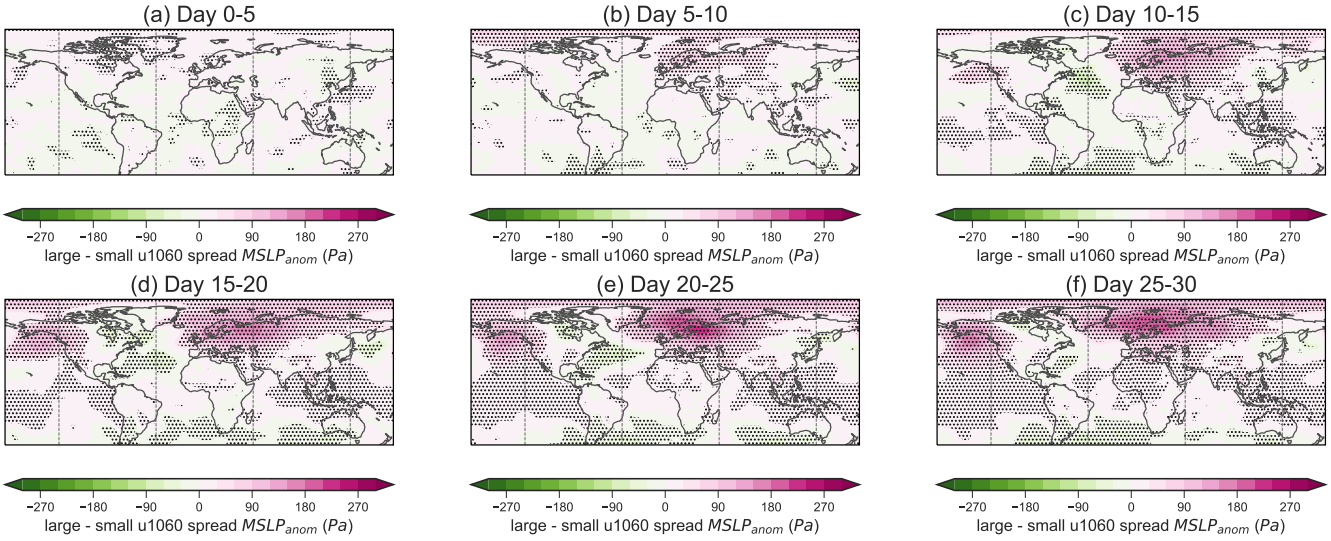

Figure 3. Difference in the evolution of composite ensemble spread of mean sea level pressure anomalies ($MSLP_{anom}$) given by hindcasts of large u1060 spread minus small u1060 spread. Differences that are significant at the 95% confidence level according to a t-test are marked by stippling.

composites expands to more regions in the tropics and subtropics as lead time increases (Figure 3c - f), including Africa at around day 25 - 30 (Figure 3f).

The regions in the troposphere where uncertainty emerges are consistent with precursor regions that are known to modulate upward wave propagation into the stratosphere, namely over the North Pacific and Northern Europe (Garfinkel et al., 2010; Barriopedro and Calvo, 2014), and over Scandinavia and the Ural mountains, regions where increased blocking frequency occurs before SSWs (Martius et al., 2009; Peings, 2019). The consistency between the identified tropospheric origins of uncertainty and the precursor regions might suggest a propagation of uncertainty from the troposphere into the stratosphere through uncertainty in upward wave propagation (Schwartz et al., 2022), associated with uncertainty in the synoptic-scale conditions located in these regions (Lee et al., 2019, 2020).

At the same time, several of these regions are known to be impacted by stratospheric forcing, e.g. after SSW events. SSW can have downward impact over the Euro-Atlantic sector, resulting in a shift of storm track position (Afargan-Gerstman and Domeisen, 2020; Maycock et al., 2020), in a change of cyclone frequency (Afargan-Gerstman et al., 2024), and in the transition of weather regimes (Charlton-Perez et al., 2018; Domeisen et al., 2020c). Hence, since SSW events occur more frequently within the first 10 days after initialization in the small u1060 spread hindcasts (not shown), the regions highlighted at longer lead times (Figure 3d - f) could also be related to downward impacts from the stratosphere.

https://doi.org/10.5194/egusphere-2024-1652
Preprint. Discussion started: 5 June 2024

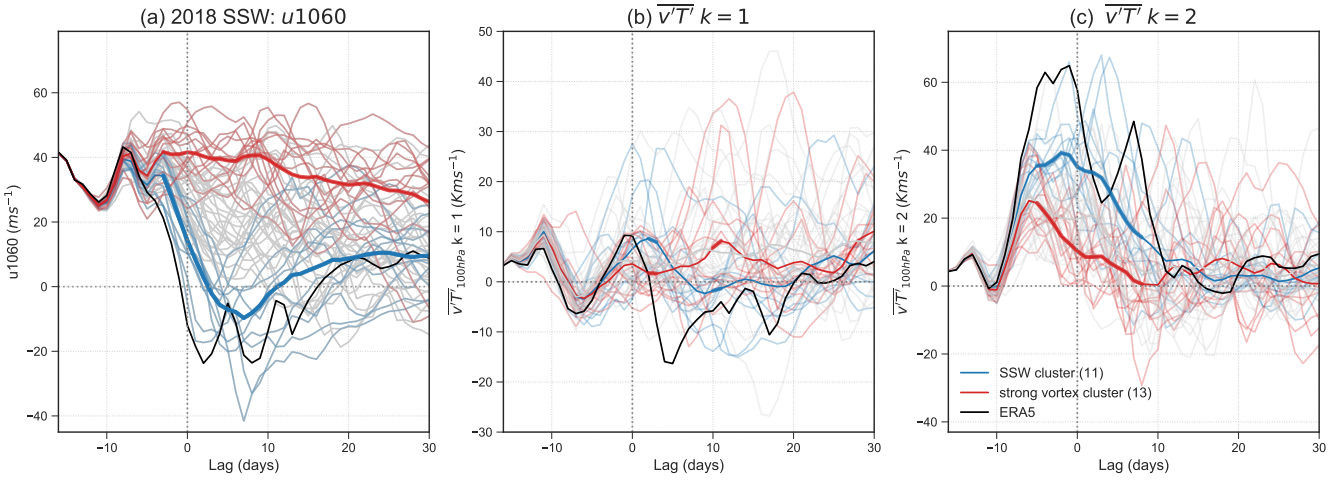

Figure 4. Ensemble plumes of (a) u1060 and $\overline{v'T'}$ at 100 hPa averaged over 45-75° N for (b) wave-1 and (c) wave-2, respectively, for the hindcast of the 2018 SSW event. Ensemble members are separated into strong vortex cluster (red) and SSW cluster (blue). The black line denotes ERA5. The vertical line denotes the central date of the SSW on February 12, 2018.

5 Development of the High Uncertainty in the 2018 SSW Prediction

A case with particularly high uncertainty in the prediction of the stratosphere was the SSW event on February 12, 2018. This case therefore represents a prime example for studying the origins of stratospheric uncertainty and their link to the troposphere. Furthermore, this event had a wide range of surface impacts (e.g. Kautz et al., 2020; Ayarzagüena et al., 2018; Hitchcock et al., 2022), while its prediction itself exhibited high uncertainty despite a range of suggested precursors, including extratropical troughs and blockings (Rao et al., 2018; Karpechko et al., 2018; Lee et al., 2019), and an MJO teleconnection (Statnaia et al., 2020).

We therefore further explore the development of uncertainty for the case study of the 2018 SSW. For this purpose we use an additional hindcast initialization with a larger number of ensemble members, initialized 16 days before the onset of the 2018 SSW event (see Methods). This initialization is selected because it includes ensemble members that successfully predict the onset of the SSW event and members that erroneously predict a strong vortex state around the time of the SSW onset, contributing to the large spread in ensemble for u1060 (Figure 4a). The selected initialization date shows a particularly extreme spread in u1060 compared to other initialization dates, with the spread increasing beyond the 95th percentile of the climatology and peaking at 7 days after the SSW onset (purple dashed line in Figure 1a). Consistent with the characteristics of the large uncertainty hindcasts discussed in Section 3, the hindcast is initialized under a strong vortex state (Figure 1b) and is associated with strong eddy heat flux around 10-20 days after initialization (Figure 1c), consistent with the occurrence of the SSW. Similar to Kautz et al. (2020), we separate the ensemble into two clusters, one with ensemble members that successfully predict the SSW (*SSW cluster*) and one that predicts a strong vortex state (*strong vortex cluster*) (Fig. 4a), to investigate the differences between the clusters that subsequently lead to different predictions of the vortex strength.

https://doi.org/10.5194/egusphere-2024-1652
Preprint. Discussion started: 5 June 2024

Before the onset of the SSW, the clusters do not differ significantly in wave-1 heat flux in the lower stratosphere, whereas they do differ significantly in wave-2 at around lag -5 (Figure 4b and c). Both clusters show an initial increase in wave-2 activity, but the wave activity of the strong vortex cluster decreases shortly after the initial increase. The observed difference between the two clusters in the wave-2 activity suggests that accurately predicting the wave-2 activity is crucial for successfully predicting the SSW, in agreement with previous studies (Karpechko et al., 2018; Rao et al., 2018; Lee et al., 2019; Statnaia et al., 2020). Although the SSW cluster on average still underestimates the wave activity as compared to reanalysis, and as a consequence the vortex deceleration, several individual ensemble members predict eddy heat fluxes comparable to reanalysis.

To further understand the origin of the difference between the clusters in wave-2 activity, we compare the differences between the clusters in terms of their respective anomalies of outgoing longwave radiation (OLR) before SSW onset (Figure 5a - b), and in mean sea level pressure (MSLP) anomalies before and after SSW onset (Figure 5c - h). Before SSW onset, for lags -14 to -1, the SSW cluster shows more enhanced convection over the Maritime Continent and more suppressed convection over parts of Africa and South America than the strong vortex cluster (Figure 5a - b). During lags -14 to -8, the SSW cluster also shows stronger MSLP anomalies that project onto the Pacific North American (PNA) pattern and a stronger positive pressure anomaly over the North Atlantic (Figure 5c). During lags -7 to -1, for the SSW cluster, the high pressure anomaly over Scandinavia amplifies and a stronger negative pressure anomaly over the North Atlantic is found (Figure 5d). This pressure dipole between Scandinavia and the North Atlantic is remarkably similar to the pattern that is identified by Kent et al. (2023) to be crucial for successfully predicting the 2013 SSW, which was also preceded by strong wave-2 flux. The simultaneous increase in pressure over Scandinavia and the North Pacific projects onto a wave-2 pattern that likely forced the upward wave-2 activity flux, as the patterns identified here in MSLP are also observed at higher pressure levels, in the upper troposphere and in the lower stratosphere (Figure A1).

The higher pressure over Scandinavia and the lower pressure over the North Atlantic in the SSW cluster as compared to the strong vortex cluster before the SSW onset (Figure 5d) persist and strengthen further after SSW onset, while the high pressure anomaly extends further towards Greenland and then spreads across the Arctic (Figure 5e-h). Starting at lag 7, the anomalies start resembling the negative phase of North Atlantic Oscillation (NAO) (Figure 5f - h). This development of the anomalies in the SSW cluster is consistent with the observed evolution of surface anomalies following the SSW event (Kautz et al., 2020; González-Alemán et al., 2022; Domeisen et al., 2020c), indicating that ensemble members that successfully capture the teleconnection from the tropics into the extratropics not only better predict the SSW but also the associated downward impacts.

6 Conclusions

The uncertainty in the prediction of the stratosphere and its origins and impacts are systematically investigated using the S2S hindcasts of the ECMWF prediction system. By separating hindcasts into those that show large uncertainty versus those that show small uncertainty in the prediction of the polar vortex strength (u1060), using ensemble spread as a measure of uncertainty, we find that hindcasts associated with large uncertainty (large u1060 spread) tend to be initialized under a strong vortex, while hindcasts associated with small uncertainty (small u1060 spread) tend to be initialized under a weak vortex.

https://doi.org/10.5194/egusphere-2024-1652
Preprint. Discussion started: 5 June 2024

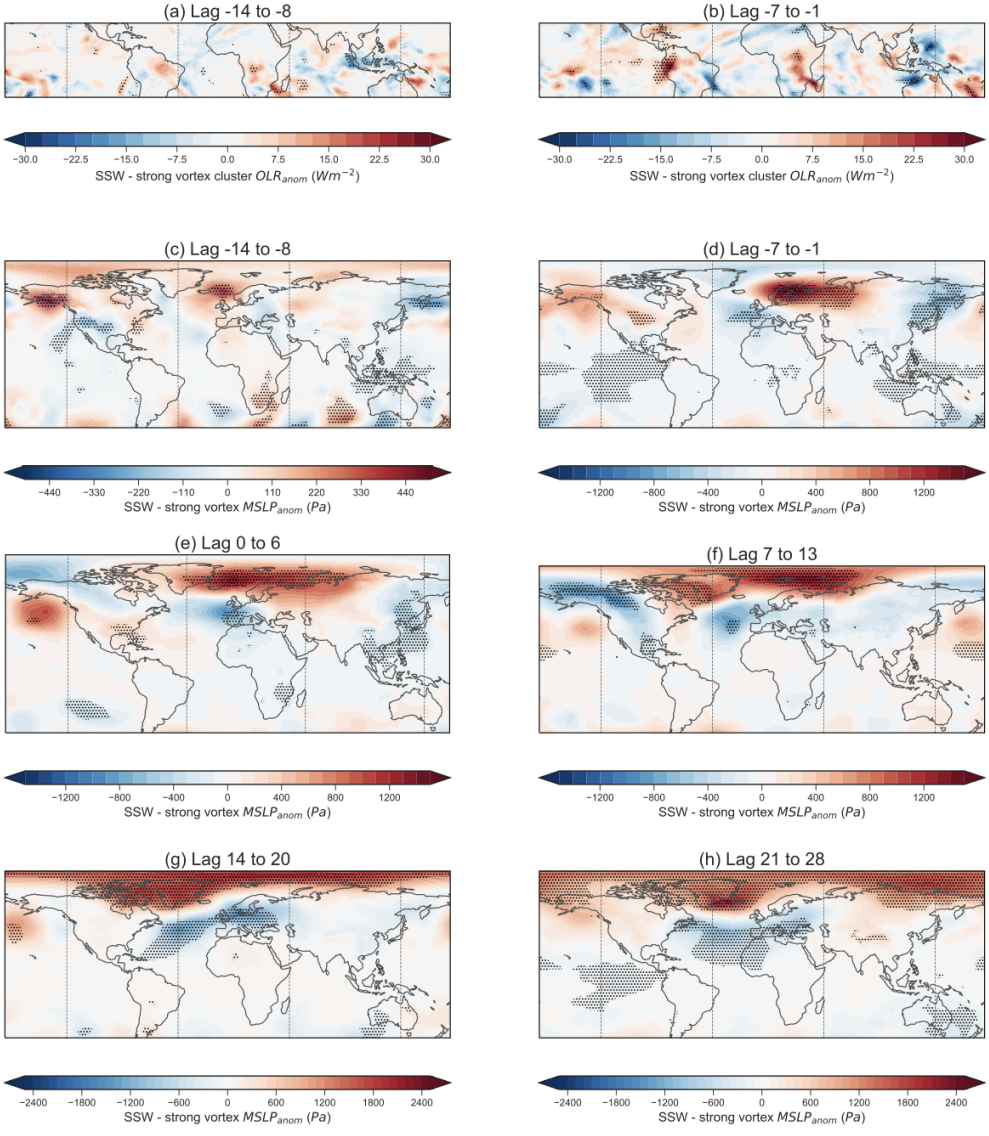

Figure 5. Difference between the SSW cluster and the strong vortex cluster in weekly averages of (a,b) outgoing longwave radiation (OLR) anomalies before SSW onset, and (c) - (h) mean sea level pressure (MSLP) anomalies before and after SSW onset for the hindcast of the 2018 SSW. Lag is given in days with respect to SSW onset. Anomalies are averaged every 7 days starting from 14 days before SSW onset (lag -14 corresponds to 2 days after initialization), for MSLP anomalies up to 28 days after SSW onset (lag 28). Stippling indicates a significant difference between the two clusters by a t-test at the 95% confidence level. Note that the upper and lower limits of the colorbars are increased from (c) to (h), with a colorbar range of $\pm$ 500Pa in (c), $\pm$ 1500Pa in (d) to (f), and $\pm$ 2500Pa in (g) and (h).

https://doi.org/10.5194/egusphere-2024-1652
Preprint. Discussion started: 5 June 2024

Large u1060 spread hindcasts are also associated with a stronger ensemble mean wave activity in the lower stratosphere and associated with larger uncertainty in the wave activity compared to small u1060 spread hindcasts.

The difference in uncertainty between the hindcasts is further linked to the troposphere. Specifically, larger uncertainty is identified over the North Pacific and Northern Europe in large u1060 spread hindcasts, where synoptic-scale variability can modulate stratospheric vortex strength (Garfinkel et al., 2010; Martius et al., 2009) and impact the prediction of the stratosphere (Kent et al., 2023). This tropospheric pattern suggests upward propagation of uncertainty from the troposphere into the stratosphere through the uncertainty associated with the synoptic-scale conditions in these precursor regions. In turn, synoptic-scale tropospheric uncertainties following stratospheric disruptions can also limit the predictability of the troposphere (González-Alemán et al., 2022), hence the identified uncertainty signal in the North Atlantic region is likely linked to both precursors and responses to stratospheric extremes.

Since it is not possible to clearly separate tropospheric precursors and responses in the analysis of uncertainty for all cases, the upward and downward coupling of uncertainty between the troposphere and the stratosphere is further explored in a hindcast of the 2018 SSW initialized 16 days before the event onset under a strong vortex. This event showed a particularly strong uncertainty in the stratosphere ahead of the event onset. The hindcast's ensemble spans from erroneously predicting a strong vortex to successfully predicting the observed SSW event. The ensemble members that successfully predict the SSW are preceded by enhanced convection over the Maritime Continent, followed by a development of an anomalously strong PNA pattern, and a development of an Atlantic trough and a high pressure anomaly over Scandinavia. These initial differences in the development of tropospheric conditions between the ensemble members lead to the subsequent difference in the development of wave-2, which results in drastically different predictions of the vortex state by the different ensemble clusters. Since the hindcast of the 2018 SSW is initialized near a record-breaking MJO phase 6 (Barrett, 2019), and since the MJO is also suggested to act as a trigger for the SSW event (Statnaia et al., 2020), this hindcast of the 2018 SSW represents an example demonstrating the propagation of uncertainty from the tropical troposphere into the stratosphere through teleconnection pathways (Straus et al., 2023; Roberts et al., 2023). The ensemble members that successfully capture the MJO teleconnection and the SSW also better capture the downward impact associated with the SSW. Therefore, this hindcast also demonstrates the extended surface prediction skill that can be gained from the successful prediction of an SSW due to its precursors.

While tropospheric variability alone cannot fully explain the uncertainties in the stratosphere, and while not all wave activity that drives SSWs has a tropospheric origin (e.g. Birner and Albers, 2017), this study highlights how uncertainties in the troposphere can contribute to uncertainty in the stratosphere, and vice versa. Thus, a better representation of the regions identified in this study can be beneficial for both tropospheric and stratospheric prediction, in agreement with the suggested precursor regions of SSWs, e.g. over the North Pacific, the North Atlantic (e.g. Martius et al., 2009; Garfinkel et al., 2010), and the tropics, for instance over the Maritime Continent for MJO teleconnections (e.g. Kang and Tziperman, 2018; Yadav et al., 2024). Model improvements for these regions, e.g. higher model resolution, improved representation of SST gradients and diabatic heating in these regions, may benefit the representation of the synoptic-scale conditions over the extratropics and, subsequently, the prediction of the stratosphere and its downward impacts.

https://doi.org/10.5194/egusphere-2024-1652
Preprint. Discussion started: 5 June 2024

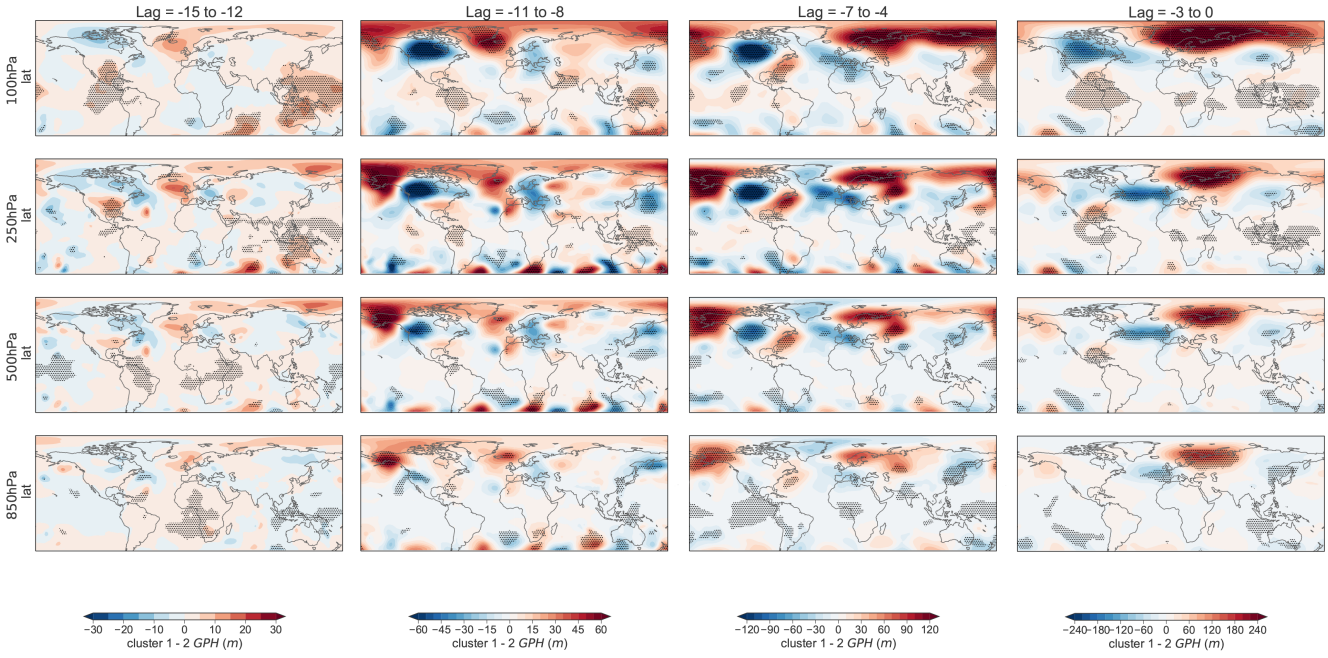

Figure A1. Difference between the SSW cluster and the strong vortex cluster in geopotential height at 100, 250, 500 and 850 hPa for the re-simulation of the 2018 SSW, averaged every 4 days starting from 1 day after initialization (lag -15) to SSW onset (lag 0). Stippling indicates a significant difference between the two clusters by a t-test at 95% confidence interval. Note that the range of the colour bars is doubled in every time step from lag -15 to -12 to lag -3 to 0.

Data availability. The ERA-Interim (Dee et al. (2011), https://cds.climate.copernicus.eu/#!/home; 2019) and ERA5 data (Hersbach et al. (2020), https://cds.climate.copernicus.eu/#!/home, 2023) are available from Copernicus Climate Change Service (C3S). The subseasonal-to-seasonal (S2S) data (Vitart et al. (2017), https://apps.ecmwf.int/datasets/data/s2s-reforecasts-instantaneous-accum-ecmf/levtype=sfc/type=cf/, 2019) is available from the ECMWF Public Dataset Service. The re-run of the hindcast data for the 2018 SSW event used in the study will be publicly available from https://doi.org/10.21957/hcmn-0572 (ECMWF (2024), https://doi.org/10.21957/hcmn-0572, 2024).

Appendix A

Author contributions. R.W. and D.D. designed the study. I.P. performed the re-run for the hindcast. R.W. performed the analysis, made the figures, and wrote the manuscript draft. R.W., D.D., G.C. and I.P. discussed the research and worked on revising the manuscript.

Competing interests. The authors declare no competing interests.

https://doi.org/10.5194/egusphere-2024-1652
Preprint. Discussion started: 5 June 2024

Acknowledgements. The work of R.W. is partly funded through ETH grant ETH-05 19-1 "How predictable are sudden stratospheric warming events?". Support from the Swiss National Science Foundation through project PP00P2_198896 to D.D., and PZ00P2_180043 to G.C. is gratefully acknowledged. The authors would like to thank Frédéric Vitart, Andrew Charlton-Perez, Hilla Afargan-Gerstman and Zheng Wu for helpful discussions regarding this work.

https://doi.org/10.5194/egusphere-2024-1652
Preprint. Discussion started: 5 June 2024

References

Afargan-Gerstman, H. and Domeisen, D. I. V.: Pacific Modulation of the North Atlantic Storm Track Response to Sudden Stratospheric Warming Events, Geophys. Res. Lett., 47, e2019GL085 007, https://doi.org/10.1029/2019GL085007, 2020.

Afargan-Gerstman, H., Büeler, D., Wulff, C. O., Sprenger, M., and Domeisen, D. I. V.: Stratospheric influence on the winter North Atlantic storm track in subseasonal reforecasts, Weather Clim. Dyn., 5, 231–249, https://doi.org/10.5194/wcd-5-231-2024, 2024.

Albers, J. R. and Birner, T.: Vortex preconditioning due to planetary and gravity waves prior to sudden stratospheric warmings, Journal of the Atmospheric Sciences, 71, 4028–4054, https://doi.org/10.1175/JAS-D-14-0026.1, 2014.

Ayarzagüena, B., Barriopedro, D., Garrido-Perez, J. M., Abalos, M., de la Cámara, A., García-Herrera, R., Calvo, N., and Ordóñez, C.: Stratospheric Connection to the Abrupt End of the 2016/2017 Iberian Drought, Geophys. Res. Lett., 45, 12,639–12,646, https://doi.org/10.1029/2018GL079802, 2018.

Baldwin, M. P. and Dunkerton, T. J.: Stratospheric Harbingers of Anomalous Weather Regimes, Science, 294, 581–584, https://doi.org/10.1126/science.1063315, 2001.

Baldwin, M. P., Ayarzagüena, B., Birner, T., Butchart, N., Butler, A. H., Charlton-Perez, A. J., Domeisen, D. I. V., Garfinkel, C. I., Garny, H., Gerber, E. P., Hegglin, M. I., Langematz, U., and Pedatella, N. M.: Sudden Stratospheric Warmings, Rev. Geophys., 59, e2020RG000 708, https://doi.org/10.1029/2020RG000708, 2021.

Barrett, B. S.: Connections between the Madden–Julian Oscillation and surface temperatures in winter 2018 over eastern North America, Atmos. Sci. Lett., 20, e869, https://doi.org/10.1002/asl.869, 2019.

Barriopedro, D. and Calvo, N.: On the Relationship between ENSO, Stratospheric Sudden Warmings, and Blocking, J. Clim., 27, 4704–4720, https://doi.org/10.1175/JCLI-D-13-00770.1, 2014.

Birner, T. and Albers, J. R.: Sudden Stratospheric Warmings and Anomalous Upward Wave Activity Flux, SOLA, 13A, 8–12, https://doi.org/10.2151/sola.13A-002, 2017.

Butler, A. H., Charlton-Perez, A., Domeisen, D. I. V., Garfinkel, C., Gerber, E. P., Hitchcock, P., Karpechko, A. Y., Maycock, A., Sigmond, M., Simpson, I., and Son, S.-W.: Sub-seasonal Predictability and the Stratosphere, in: Sub-seasonal to Seasonal Prediction, edited by Robertson, A. W. and Vitart, F., chap. 11, p. 585, Elsevier, Amsterdam, Netherlands, https://doi.org/10.1016/C2016-0-01594-2, 2018.

Büeler, D., Beerli, R., Wernli, H., and Grams, C. M.: Stratospheric influence on ECMWF sub-seasonal forecast skill for energy-industry-relevant surface weather in European countries, Q. J. R. Meteorolog. Soc., 146, 3675–3694, https://doi.org/10.1002/qj.3866, 2020.

Charlton, A. J., O'Neill, A., Lahoz, W. A., and Massacand, A. C.: Sensitivity of tropospheric forecasts to stratospheric initial conditions, Q. J. R. Meteorolog. Soc., 130, 1771–1792, https://doi.org/10.1256/qj.03.167, 2004.

Charlton-Perez, A. J., Ferranti, L., and Lee, R. W.: The influence of the stratospheric state on North Atlantic weather regimes, Q. J. R. Meteorolog. Soc., 144, 1140–1151, https://doi.org/10.1002/qj.3280, 2018.

Charney, J. G. and Drazin, P. G.: Propagation of planetary-scale disturbances from the lower into the upper atmosphere, J. Geophys. Res., 66, 83–109, https://doi.org/10.1029/JZ066i001p00083, 1961.

Chwat, D., Garfinkel, C. I., Chen, W., and Rao, J.: Which Sudden Stratospheric Warming Events Are Most Predictable?, J. Geophys. Res. Atmos., 127, e2022JD037 521, https://doi.org/10.1029/2022JD037521, 2022.

Dee, D. P., Uppala, S. M., Simmons, A. J., Berrisford, P., Poli, P., Kobayashi, S., Andrae, U., Balmaseda, M. A., Balsamo, G., Bauer, P., Bechtold, P., Beljaars, A. C. M., van de Berg, L., Bidlot, J., Bormann, N., Delsol, C., Dragani, R., Fuentes, M., Geer, A. J., Haimberger, L., Healy, S. B., Hersbach, H., Hólm, E. V., Isaksen, L., Kållberg, P., Köhler, M., Matricardi, M., McNally, A. P., Monge-Sanz, B. M., Mor-

https://doi.org/10.5194/egusphere-2024-1652
Preprint. Discussion started: 5 June 2024

crette, J.-J., Park, B.-K., Peubey, C., de Rosnay, P., Tavolato, C., Thépaut, J.-N., and Vitart, F.: The ERA-Interim reanalysis: configuration and performance of the data assimilation system, Q. J. R. Meteorolog. Soc., 137, 553–597, https://doi.org/10.1002/qj.828, 2011.

Domeisen, D. I., Butler, A. H., Charlton-Perez, A. J., Ayarzagüena, B., Baldwin, M. P., Dunn-Sigouin, E., Furtado, J. C., Garfinkel, C. I., Hitchcock, P., Karpechko, A. Y., Kim, H., Knight, J., Lang, A. L., Lim, E.-P., Marshall, A., Roff, G., Schwartz, C., Simpson, I. R., Son, S.-W., and Taguchi, M.: The Role of the Stratosphere in Subseasonal to Seasonal Prediction: 1. Predictability of the Stratosphere, J. Geophys. Res.-Atmos., 125, e2019JD030 920, https://doi.org/10.1029/2019JD030920, 2020a.

Domeisen, D. I. V. and Butler, A. H.: Stratospheric drivers of extreme events at the Earth's surface, Commun. Earth Environ., 1, e2019JD030 923, https://doi.org/10.1038/s43247-020-00060-z, 2020.

Domeisen, D. I. V., Butler, A. H., Charlton-Perez, A. J., Ayarzagüena, B., Baldwin, M. P., Dunn-Sigouin, E., Furtado, J. C., Garfinkel, C. I., Hitchcock, P., Karpechko, A. Y., Kim, H., Knight, J., Lang, A. L., Lim, E.-P., Marshall, A., Roff, G., Schwartz, C., Simpson, I. R., Son, S.-W., and Taguchi, M.: The Role of the Stratosphere in Subseasonal to Seasonal Prediction: 2. Predictability Arising From Stratosphere-Troposphere Coupling, J. Geophys. Res.-Atmos., 125, e2019JD030 923, https://doi.org/10.1029/2019JD030923, 2020b.

Domeisen, D. I. V., Grams, C. M., and Papritz, L.: The role of North Atlantic–European weather regimes in the surface impact of sudden stratospheric warming events, Weather Clim. Dyn., 1, 373–388, https://doi.org/10.5194/wcd-1-373-2020, 2020c.

ECMWF: 2018 SSW S2S hindcast dataset, https://doi.org/10.21957/hcmn-0572, 2024.

Ferranti, L., Magnusson, L., Vitart, F., and Richardson, D. S.: How far in advance can we predict changes in large-scale flow leading to severe cold conditions over Europe?, Q. J. R. Meteorolog. Soc., 144, 1788–1802, https://doi.org/10.1002/qj.3341, 2018.

Garfinkel, C. I., Hartmann, D. L., and Sassi, F.: Tropospheric Precursors of Anomalous Northern Hemisphere Stratospheric Polar Vortices, J. Clim., 23, 3282–3299, https://doi.org/10.1175/2010JCLI3010.1, 2010.

Garfinkel, C. I., Feldstein, S. B., Waugh, D. W., Yoo, C., and Lee, S.: Observed connection between stratospheric sudden warmings and the Madden-Julian Oscillation, Geophys. Res. Lett., 39, https://doi.org/10.1029/2012GL053144, 2012.

Garfinkel, C. I., Benedict, J. J., and Maloney, E. D.: Impact of the MJO on the boreal winter extratropical circulation, Geophys. Res. Lett., 41, 6055–6062, https://doi.org/10.1002/2014GL061094, 2014.

González-Alemán, J. J., Grams, C. M., Ayarzagüena, B., Zurita-Gotor, P., Domeisen, D. I., Gómara, I., Rodríguez-Fonseca, B., and Vitart, F.: Tropospheric role in the predictability of the surface impact of the 2018 sudden stratospheric warming event, Geophysical Research Letters, 49, e2021GL095 464, 2022.

Hersbach, H., Bell, B., Berrisford, P., Hirahara, S., Horányi, A., Muñoz-Sabater, J., Nicolas, J., Peubey, C., Radu, R., Schepers, D., Simmons, A., Soci, C., Abdalla, S., Abellan, X., Balsamo, G., Bechtold, P., Biavati, G., Bidlot, J., Bonavita, M., De Chiara, G., Dahlgren, P., Dee, D., Diamantakis, M., Dragani, R., Flemming, J., Forbes, R., Fuentes, M., Geer, A., Haimberger, L., Healy, S., Hogan, R. J., Hólm, E., Janisková, M., Keeley, S., Laloyaux, P., Lopez, P., Lupu, C., Radnoti, G., de Rosnay, P., Rozum, I., Vamborg, F., Villaume, S., and Thépaut, J.-N.: The ERA5 global reanalysis, Q. J. R. Meteorolog. Soc., 146, 1999–2049, https://doi.org/10.1002/qj.3803, 2020.

Hitchcock, P. and Shepherd, T. G.: Zonal-Mean Dynamics of Extended Recoveries from Stratospheric Sudden Warmings, J. Atmos. Sci., 70, 688–707, https://doi.org/10.1175/JAS-D-12-0111.1, 2013.

Hitchcock, P., Butler, A., Charlton-Perez, A., Garfinkel, C. I., Stockdale, T., Anstey, J., Mitchell, D., Domeisen, D. I. V., Wu, T., Lu, Y., Mastrangelo, D., Malguzzi, P., Lin, H., Muncaster, R., Merryfield, B., Sigmond, M., Xiang, B., Jia, L., Hyun, Y.-K., Oh, J., Specq, D., Simpson, I. R., Richter, J. H., Barton, C., Knight, J., Lim, E.-P., and Hendon, H.: Stratospheric Nudging And Predictable Surface Impacts (SNAPSI): a protocol for investigating the role of stratospheric polar vortex disturbances in subseasonal to seasonal forecasts, Geosci. Model Dev., 15, 5073–5092, https://doi.org/10.5194/gmd-15-5073-2022, 2022.

https://doi.org/10.5194/egusphere-2024-1652
Preprint. Discussion started: 5 June 2024

Kang, W. and Tziperman, E.: The MJO-SSW Teleconnection: Interaction Between MJO-Forced Waves and the Midlatitude Jet, Geophys. Res. Lett., 45, 4400–4409, https://doi.org/10.1029/2018GL077937, 2018.

Karpechko, A. Y., Charlton-Perez, A., Balmaseda, M., Tyrrell, N., and Vitart, F.: Predicting Sudden Stratospheric Warming 2018 and Its Climate Impacts With a Multimodel Ensemble, Geophysical Research Letters, 45, 513–538, https://doi.org/10.1029/2018GL081091, 2018.

Kautz, L.-A., Polichtchouk, I., Birner, T., Garny, H., and Pinto, J. G.: Enhanced extended-range predictability of the 2018 late-winter Eurasian cold spell due to the stratosphere, Q. J. R. Meteorolog. Soc., 146, 1040–1055, https://doi.org/10.1002/qj.3724, 2020.

Kent, C., Scaife, A. A., Seviour, W. J. M., Dunstone, N., Smith, D., and Smout-Day, K.: Identifying Perturbations That Tipped the Stratosphere Into a Sudden Warming During January 2013, Geophys. Res. Lett., 50, e2023GL106 288, https://doi.org/10.1029/2023GL106288, 2023.

Kim, H., Son, S.-W., Kim, H., Seo, K.-H., and Kang, M.-J.: MJO Influence on Subseasonal-to-Seasonal Prediction in the Northern Hemisphere Extratropics, J. Clim., 36, 7943–7956, https://doi.org/10.1175/JCLI-D-23-0139.1, 2023.

Lawrence, Z. D., Abalos, M., Ayarzagüena, B., Barriopedro, D., Butler, A. H., Calvo, N., de la Cámara, A., Charlton-Perez, A., Domeisen, D. I. V., Dunn-Sigouin, E., García-Serrano, J., Garfinkel, C. I., Hindley, N. P., Jia, L., Jucker, M., Karpechko, A. Y., Kim, H., Lang, A. L., Lee, S. H., Lin, P., Osman, M., Palmeiro, F. M., Perlwitz, J., Polichtchouk, I., Richter, J. H., Schwartz, C., Son, S.-W., Statnaia, I., Taguchi, M., Tyrrell, N. L., Wright, C. J., and Wu, R. W.-Y.: Quantifying stratospheric biases and identifying their potential sources in subseasonal forecast systems, Weather Clim. Dyn., 3, 977–1001, https://doi.org/10.5194/wcd-3-977-2022, 2022.

Lee, S. H., Charlton-Perez, A. J., Furtado, J. C., and Woolnough, S. J.: Abrupt Stratospheric Vortex Weakening Associated With North Atlantic Anticyclonic Wave Breaking, Journal of Geophysical Research: Atmospheres, 124, 8563–8575, https://doi.org/10.1029/2019JD030940, 2019.

Lee, S. H., Charlton-Perez, A. J., Furtado, J. C., and Woolnough, S. J.: Representation of the Scandinavia–Greenland pattern and its relationship with the polar vortex in S2S forecast models, Q. J. R. Meteorolog. Soc., 146, 4083–4098, https://doi.org/10.1002/qj.3892, 2020.

Limpasuvan, V., Thompson, D. W. J., and Hartmann, D. L.: The Life Cycle of the Northern Hemisphere Sudden Stratospheric Warmings, J. Clim., 17, 2584–2596, https://doi.org/10.1175/1520-0442(2004)017<2584:TLCOTN>2.0.CO;2, 2004.

Limpasuvan, V., Hartmann, D. L., Thompson, D. W. J., Jeev, K., and Yung, Y. L.: Stratosphere-troposphere evolution during polar vortex intensification, J. Geophys. Res. Atmos., 110, https://doi.org/10.1029/2005JD006302, 2005.

Martius, O., Polvani, L. M., and Davies, H. C.: Blocking precursors to stratospheric sudden warming events, Geophys. Res. Lett., 36, https://doi.org/10.1029/2009GL038776, 2009.

Matsuno, T.: Vertical Propagation of Stationary Planetary Waves in the Winter Northern Hemisphere, J. Atmos. Sci., 27, 871–883, https://doi.org/10.1175/1520-0469(1970)027<0871:VPOSPW>2.0.CO;2, 1970.

Maycock, A. C., Masukwedza, G. I. T., Hitchcock, P., and Simpson, I. R.: A Regime Perspective on the North Atlantic Eddy-Driven Jet Response to Sudden Stratospheric Warmings, J. Clim., 33, 3901–3917, https://doi.org/10.1175/JCLI-D-19-0702.1, 2020.

Peings, Y.: Ural Blocking as a driver of early winter stratospheric warmings, Geophysical Research Letters, pp. 2019GL082 097–18, 2019.

Portal, A., Ruggieri, P., Palmeiro, F. M., García-Serrano, J., Domeisen, D. I. V., and Gualdi, S.: Seasonal prediction of the boreal winter stratosphere, Clim. Dyn., 58, 2109–2130, https://doi.org/10.1007/s00382-021-05787-9, 2022.

Rao, J., Ren, R., Chen, H., Yu, Y., and Zhou, Y.: The Stratospheric Sudden Warming Event in February 2018 and its Prediction by a Climate System Model, J. Geophys. Res. Atmos., 123, 13,332–13,345, https://doi.org/10.1029/2018JD028908, 2018.

https://doi.org/10.5194/egusphere-2024-1652
Preprint. Discussion started: 5 June 2024

Roberts, C. D., Balmaseda, M. A., Ferranti, L., and Vitart, F.: Euro-Atlantic Weather Regimes and Their Modulation by Tropospheric and Stratospheric Teleconnection Pathways in ECMWF Reforecasts, Mon. Weather Rev., 151, 2779–2799, https://doi.org/10.1175/MWR-D-22-0346.1, 2023.

Scaife, A. A., Karpechko, A. Yu., Baldwin, M. P., Brookshaw, A., Butler, A. H., Eade, R., Gordon, M., MacLachlan, C., Martin, N., Dunstone, N., and Smith, D.: Seasonal winter forecasts and the stratosphere, Atmos. Sci. Lett., 17, 51–56, https://doi.org/10.1002/asl.598, 2016.

Schwartz, C. and Garfinkel, C. I.: Troposphere-Stratosphere Coupling in Subseasonal-to-Seasonal Models and Its Importance for a Realistic Extratropical Response to the Madden-Julian Oscillation, J. Geophys. Res. Atmos., 125, e2019JD032 043, https://doi.org/10.1029/2019JD032043, 2020.

Schwartz, C., Garfinkel, C. I., Yadav, P., Chen, W., and Domeisen, D. I. V.: Stationary wave biases and their effect on upward troposphere–stratosphere coupling in sub-seasonal prediction models, Weather Clim. Dyn., 3, 679–692, https://doi.org/10.5194/wcd-3-679-2022, 2022.

Sigmond, M., Scinocca, J. F., Kharin, V. V., and Shepherd, T. G.: Enhanced seasonal forecast skill following stratospheric sudden warmings, Nat. Geosci., 6, 98–102, https://doi.org/10.1038/ngeo1698, 2013.

Simpson, I. R., Blackburn, M., and Haigh, J. D.: The role of eddies in driving the tropospheric response to stratospheric heating perturbations, Journal of the Atmospheric Sciences, 66, 1347–1365, https://doi.org/10.1175/2008JAS2758.1, 2009.

Smith, K. L. and Kushner, P. J.: Linear interference and the initiation of extratropical stratosphere-troposphere interactions, J. Geophys. Res. Atmos., 117, https://doi.org/10.1029/2012JD017587, 2012.

Son, S.-W., Kim, H., Song, K., Kim, S.-W., Martineau, P., Hyun, Y.-K., and Kim, Y.: Extratropical Prediction Skill of the Subseasonal-to-Seasonal (S2S) Prediction Models, J. Geophys. Res. Atmos., 125, e2019JD031 273, https://doi.org/10.1029/2019JD031273, 2020.

Stan, C. and Straus, D. M.: Stratospheric predictability and sudden stratospheric warming events, J. Geophys. Res. Atmos., 114, https://doi.org/10.1029/2008JD011277, 2009.

Stan, C., Zheng, C., Chang, E. K.-M., Domeisen, D. I. V., Garfinkel, C. I., Jenney, A. M., Kim, H., Lim, Y.-K., Lin, H., Robertson, A., Schwartz, C., Vitart, F., Wang, J., and Yadav, P.: Advances in the Prediction of MJO Teleconnections in the S2S Forecast Systems, Bull. Am. Meteorol. Soc., 103, E1426–E1447, https://doi.org/10.1175/BAMS-D-21-0130.1, 2022.

Statnaia, I. A., Karpechko, A. Y., and Järvinen, H. J.: Mechanisms and predictability of sudden stratospheric warming in winter 2018, Weather Clim. Dyn., 1, 657–674, https://doi.org/10.5194/wcd-1-657-2020, 2020.

Straus, D. M., Domeisen, D. I. V., Lock, S.-J., Molteni, F., and Yadav, P.: Intrinsic predictability limits arising from Indian Ocean Madden–Julian oscillation (MJO) heating: effects on tropical and extratropical teleconnections, Weather Clim. Dyn., 4, 1001–1018, https://doi.org/10.5194/wcd-4-1001-2023, 2023.

Taguchi, M.: Comparison of Subseasonal-to-Seasonal Model Forecasts for Major Stratospheric Sudden Warmings, Journal of Geophysical Research: Atmospheres, 123, 231–10, https://doi.org/10.1029/2018JD028755, 2018.

Tripathi, O. P., Baldwin, M., Charlton-Perez, A., Charron, M., Eckermann, S. D., Gerber, E., Harrison, R. G., Jackson, D. R., Kim, B.-M., Kuroda, Y., Lang, A., Mahmood, S., Mizuta, R., Roff, G., Sigmond, M., and Son, S.-W.: The predictability of the extratropical stratosphere on monthly time-scales and its impact on the skill of tropospheric forecasts, Q. J. R. Meteorolog. Soc., 141, 987–1003, https://doi.org/10.1002/qj.2432, 2015a.

Tripathi, O. P., Charlton-Perez, A., Sigmond, M., and Vitart, F.: Enhanced long-range forecast skill in boreal winter following stratospheric strong vortex conditions, Environ. Res. Lett., 10, 104 007, https://doi.org/10.1088/1748-9326/10/10/104007, 2015b.

Vitart, F., Ardilouze, C., Bonet, A., Brookshaw, A., Chen, M., Codorean, C., Déqué, M., Ferranti, L., Fucile, E., Fuentes, M., Hendon, H., Hodgson, J., Kang, H. S., Kumar, A., Lin, H., Liu, G., Liu, X., Malguzzi, P., Mallas, I., Manoussakis, M., Mastrangelo, D., MacLachlan, C.,

https://doi.org/10.5194/egusphere-2024-1652
Preprint. Discussion started: 5 June 2024

McLean, P., Minami, A., Mladek, R., Nakazawa, T., Najm, S., Nie, Y., Rixen, M., Robertson, A. W., Ruti, P., Sun, C., Takaya, Y., Tolstykh, M., Venuti, F., Waliser, D., Woolnough, S., Wu, T., Won, D. J., Xiao, H., Zaripov, R., and Zhang, L.: The subseasonal to seasonal (S2S) prediction project database, Bulletin of the American Meteorological Society, 98, 163–173, https://doi.org/10.1175/BAMS-D-16-0017.1, 2017.

Wu, R. W.-Y., Wu, Z., and Domeisen, D. I. V.: Differences in the sub-seasonal predictability of extreme stratospheric events, Weather Clim. Dyn., 3, 755–776, https://doi.org/10.5194/wcd-3-755-2022, 2022.

Yadav, P., Garfinkel, C. I., and Domeisen, D. I. V.: The Role of the Stratosphere in Teleconnections Arising From Fast and Slow MJO Episodes, Geophys. Res. Lett., 51, e2023GL104 826, https://doi.org/10.1029/2023GL104826, 2024.